Journal of the Korean Nuclear Society
Volume 32, Number 6, pp.595~604, December, 2000

Flow-Accelerated Corrosion Behavior of SA106 Gr.C Steel in Alkaline Solution Characterized by Rotating Cylinder Electrode

Jun Hwan Kim and In Sup Kim
Korea Advanced Institute of Science and Technology,
373-1 Kusong-dong, Yusong-gu, Taejon, Korea, 305-701
iskim@sorak.kaist.ac.kr

(Received April 20, 2000)

Abstract

Flow-Accelerated Corrosion behavior of SA106 Gr.C steel in room temperature alkaline solution simulating the CANDU primary water condition was studied using Rotating Cylinder Electrode. Systems of RCE were set up and electrochemical parameters were applied at various rotating speeds. Corrosion current density decreased up to pH 10.4 then it increased rapidly at higher pH. This is due to the increasing tendency of cathodic and anodic exchange half-cell current. Corrosion potential shifted slightly upward with rotating velocity. Passive film was formed from pH 9.8 by the mechanism of step oxidation and the subsequent precipitation of ferrous species into hydroxyl compound. Above pH 10.4, the film formation process was active and the film became stable. Corrosion current density showed increment in pH 6.98 with the rotating velocity, while it soon saturated from 1000 rpm above pH 9.8. This seems that activation process which represents formation of passive film on the bare metal surface controls the entire corrosion process

Key Words : Flow-Accelerated Corrosion (FAC), alkaline solution, corrosion rate, Rotating Cylinder Electrode (RCE), low alloy steel, activation process, passive film

1. Introduction

Flow-Accelerated Corrosion (FAC) is a process where protective oxide layer on carbon or low-alloy steel dissolves into a stream of flowing water or a water-steam mixture. The layer becomes thinner and less protective. Eventually a steady state is reached where the dissolution and removal rates are equal, and the stable corrosion rates are maintained. A thinned component would typically fail due to overstress from operating pressure or abrupt changes in conditions such as waterhammer, start-up loading, and so on. It first appeared in a nuclear power plant by the condensate system failure in Surry, resulted in several casualties. After the accident, numerous components, such as feedwater system in Trojan, moisture separate drains failure at Millstone 3

Unit, suffered problem of FAC and it is now considered as one of the main degradation stressors on secondary piping in PWR, along with high cycle fatigue [1,2]. Thus FAC-based life management systems in secondary piping, such as CHECWORKS code in Electric Power Research Institute(EPRI), WATHEC code in KWU-Siemens, and BRT - CICERO in Electricite de France(EDF), have been developed since the accident of Surry.

Whereas FAC problems in CANDU primary heat transport system were not emerged because its water chemistry seemed to be far from corrosion until Point Lepreau feeder leak accident happened. After AECL's recommendation of periodic monitoring feeder wall thickness, Gentilly-2, Embalse, Pickering, and Wolsong reported the same problem related to FAC [3]. And it is recognized as potential hazard in CANDU primary heat transport system because corrosion parameters are not fully investigated in simulated CANDU environments, not to mention of clarifying FAC mechanisms and proposing mitigation strategies in operating power plant.

The objectives in this study are to observe FAC behavior of low alloy piping steel in simulated CANDU primary coolant condition using rotating cylinder electrode, and to study on the corrosion phenomena with the flow rate and solution pH in terms of initial passive layer formation.

2. Experimental Procedures

2.1. Corrosion Experiment

To observe fundamental electrochemical parameters in CANDU primary coolant conditions, polarization test (potentiodynamic test) was conducted. Electrochemical data were measured through the three-electrode system using EG&G model 362 scanning potentiostat. Scan rate was 0.5mV/sec. The reference electrode and auxiliary electrode were Saturated Calomel Electrode and graphite, respectively. Water chemistry condition in this study simulated the CANDU primary water coolant conditions. Thus experimental solution was composed of distilled water and lithium hydroxide (LiOH). All conditions in this study were de-aerated by nitrogen gas injection for 3 hours and pH of the solution was selected as 9.84, 10.4, 10.6, 11.06, and 11.83 by the step titration of 1M LiOH. To obtain better conductivity and alleviate large IR drop across pure water, dilute PWR primary water condition was introduced to neutral solution in pH 6.96 [4]. Test material used in this study is SA106 Gr.C steel with similar chromium content and microstructure to SA106 Gr.B steel which is actually used as feeder materials. Corrosion current density was measured through both Tafel extrapolation and linear polarization method near the corrosion potential, in which governing equation could be expressed as follows;

$$E = \beta \log i + c \qquad \text{(Tafel Extrapolation method)}$$

$$i_{corr} = \frac{\beta_a \cdot \beta_c}{2.303(\beta_a + \beta_c)} \cdot \frac{1}{R} \qquad \text{(Linear polarization method)}$$

where β : Tafel constant (a, c denote anodic and cathodic part)

R : slope of potential and current around corrosion potential

2.2. Rotating Cylinder Electrode (RCE) Experiment.

RCE is a device which contains cylindrical electrode in corrosion cell to investigate the effect of flow on the corrosion behavior by the circumferential flow of the rotating cylinder. Initially the device was used in chemical engineering for the purpose of electrorefining

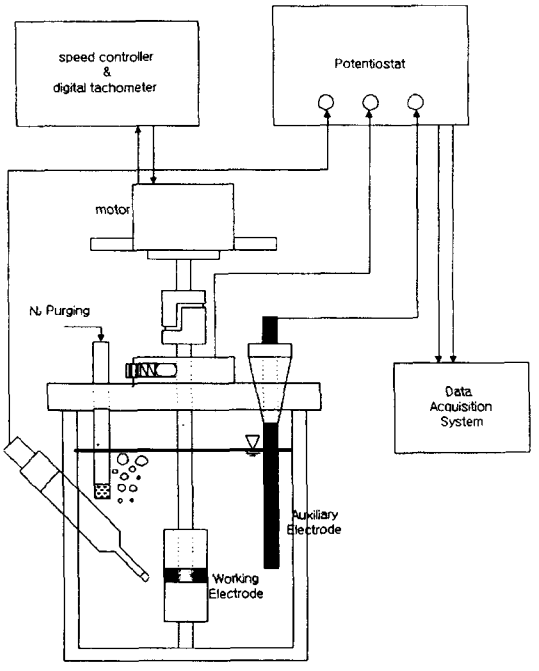

Fig. 1. Schematic Illustration of RCE Setups

and electrodeposition study, it is now applied in FAC field because it is cost-effective, produces turbulent flow easily, generates reproducible uniform current distribution, and so on [5]. Fig. 1 shows a schematic diagram of RCE setup. Spring-pushed bridge was contacted to rotating bar for the extraction of electric signal and application of external potential into working electrode. To diminish IR drop variation during the entire test period, a reference electrode was inserted in an inclined position and fixed as close as possible to maintain constant distance between electrodes. All specimens were ground with emery paper, and finally polished down to the 6μm grit, de-greased by acetone and cathodically charged in -1,000mV(SCE) to remove oxide on the specimen prior to the experiment. The area of working electrode was 4.71cm^2. The working electrode was taken from

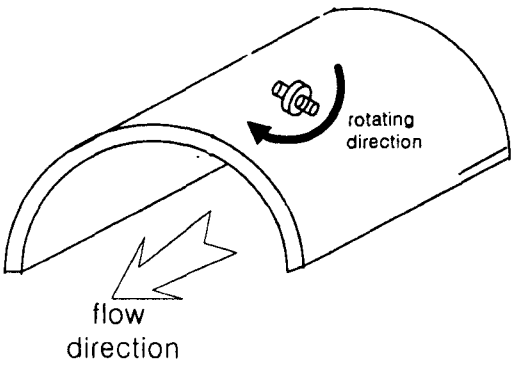

Fig. 2. Metallographic Orientation of RCE Specimen

the orientation in which the coolant actually flowed, as implied in Fig. 2. Teflon cylinder was attached, whose thickness is ten times larger than working electrode in order to avoid edge effect, that is, the distortion of flow near the edge of the rotating electrode. Motor used in this study was VEXTA FBL-220A model. Corrosion potential in this study could be decided at the point where anodic (i_a) and cathodic half-cell current density (i_c) are equal. Corrosion current density was measured through linear polarization method.

3. Results and Discussions

3.1. Polarization Results

Fig. 3 shows potentiodynamic result with increasing pH. Metal simply dissolves in the anodic potential regime at neutral condition, showing no passive film formation on the surface. Meanwhile, it was formed in an incomplete manner from pH 9.84. Above pH 10.4, the film appeared stable from the observation of the passivation potential and the average film current density. Average cathodic Tafel slope is two times of anodic Tafel slope by the value of -258.9mV

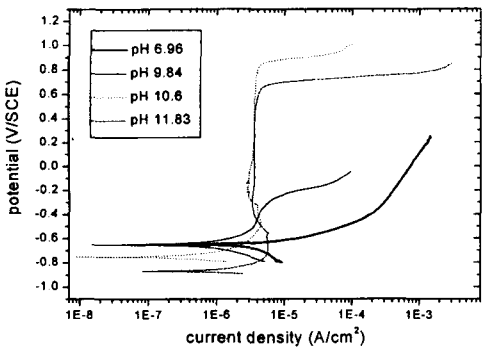

(a)

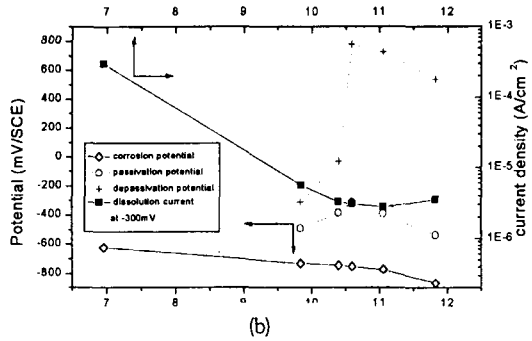

(b)

Fig. 3. Electrochemical Results of SA106 Gr.C Steel in Static Condition

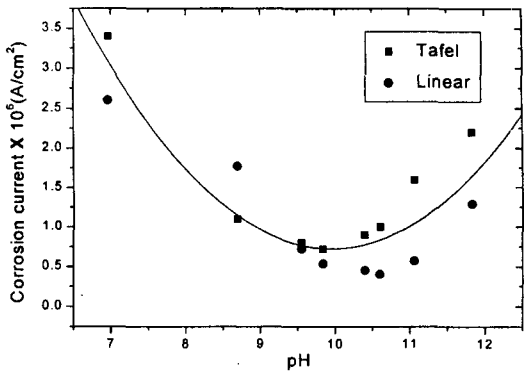

Fig. 4. Results of Tafel and Linear Polarization with the Different of pH in Static Condition

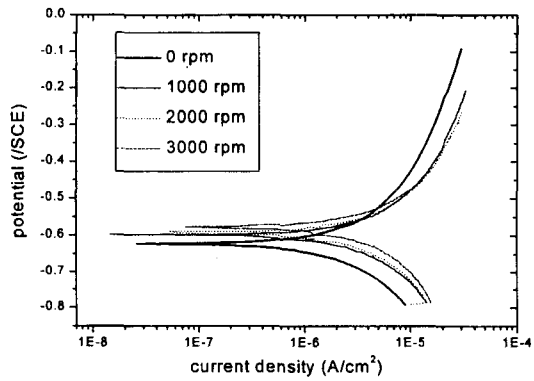

Fig. 5. Results of RCE in Neutral Solution

and 104.6mV, to which charge transfer equivalents are inversely proportional. Fig. 4 shows the plot of corrosion current density calculated both by Tafel and linear polarization with pH. In this figure, they are more or less of parabolic shapes with the local minima at pH 10.4. This seems to be inconsistent with the conventional weight loss data of mild steel in high pH solutions [6]. Such an increasing tendency of corrosion current density above pH 10.4 can be explained by the electrochemical nature of alkaline corrosion [7], which governed the kinetic reaction of iron electrode like;

Anodic half-cell reaction :

$$Fe + 2OH^- \rightarrow Fe(OH)_2 + 2e^-$$

$$i_a = 2k_a F[OH^-]^{1.5} \exp\{FE/RT\}$$

Cathodic half-cell reaction :

$$H_2O + e^- \rightarrow \tfrac{1}{2}H_2 + OH^-$$

$$i_c = -k_c F[H_2O]\exp\{-FE/2RT\}$$

Where k_a, and k_c denote anodic and cathodic reaction rate constant. In case of increasing hydroxyl ion concentration, each anodic and cathodic half-cell current density increases such that entire corrosion exchange current density

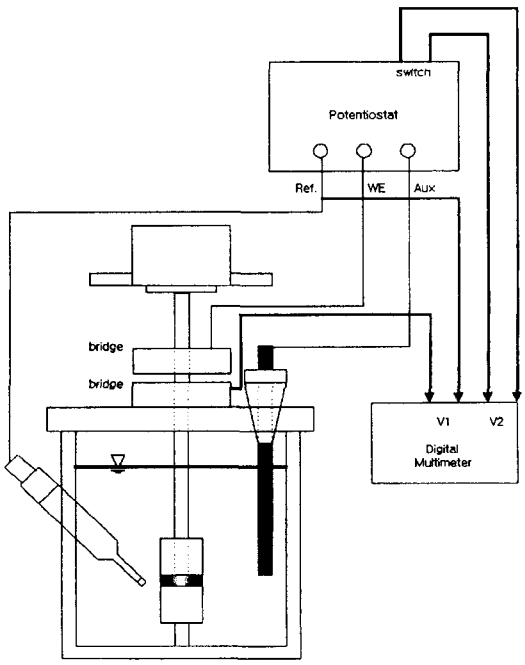

(a)

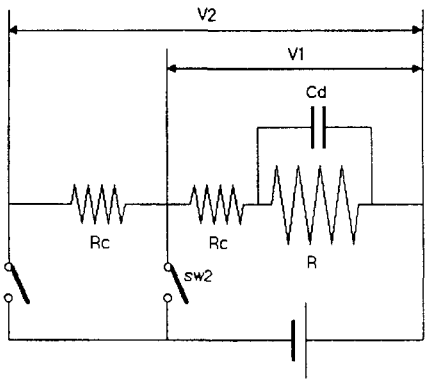

(b)

Fig. 6. (a) Bypass (b) Equivalent Circuit for the Effect of Contact Resistance

increases on the bare metal surface near the corrosion potential, in which both anodic and cathodic reaction may compete. When the passive film is formed, such a current transient will drop to a stable value, which causes suppressing metal loss.

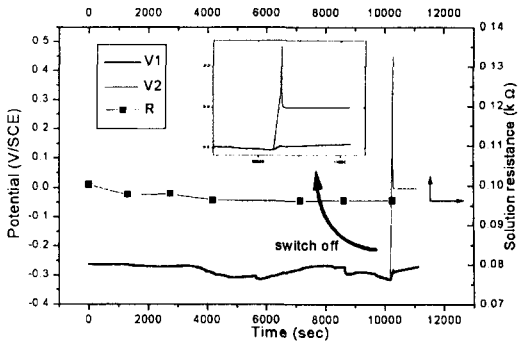

Fig. 7. Effect of Contact Resistance in Given RCE System. Solution pH was Set to 12.1

3.2. RCE Results

Fig. 5 is the polarization curve versus rotating velocity in neutral solution. It was observed that both the corrosion potential and the dissolution current density at anodic regime augment with rotating velocity. The upward shift of corrosion potential with rotating velocity may be due to the migration of reducing agent on the metal electrode more easily with the turbulent flow [8].

A bypass circuit has been installed as in Fig. 6(a) to investigate if contact resistance and related thermal resistance between the bridge and rotating bar can affect the total current in given RCE system. Their equivalent circuit is modeled in Fig. 6(b). Result of potential value at each junction point is shown in Fig. 7. It can be shown that V_1 which exerts driving force of overall corrosion process and V_2 which represents open-circuit potential are almost equal during the test period. Thus it was confirmed that effect of such resistance on the entire corrosion current is negligible compared to the polarization resistance.

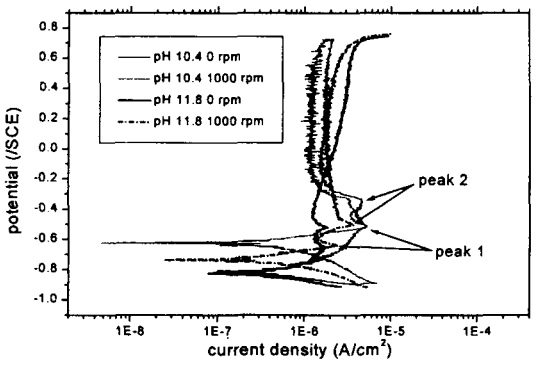

Fig. 8. Polarization Curves in pH 10. 4 and 11.8 at Rotating Velocities

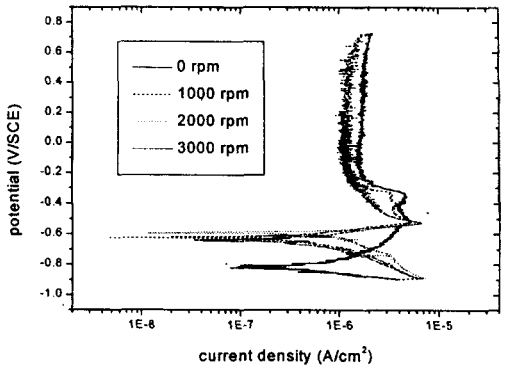

Fig. 9. Polarization Curve of pH 10.4 with Rotating Velocity

3.3. Effect of pH

Fig. 8 shows polarization curve with increasing pH. As seen from this figure, two characterized peaks appeared at the anodic active-passive transition potential. Similar results were reported by Zhou who studied corrosion behavior of mild steel at concentrated NaOH solutions [9]. He proposed that first anodic peak combined three parallel processes, which were composed of active dissolution of iron to a soluble bi-valent ion product of $HFeO_2^-$, formation of a surface layer and passive film, and formation of a soluble tri-valent iron species of FeO_2^- prior to the onset of passivation, and second anodic process represented the oxidation of the Fe_3O_4 magnetite film to Fe_2O_3, FeO_2^-. Proposed electrode reactions at each anodic potential based on our experimental results are as follows [9, 10] ;

First peak :

$$E(\text{vs. SHE}) = 0.925 - 0.114\text{pH}$$

$$3Fe(OH)_2 + 2OH^- \rightarrow Fe_3O_4 + 4H_2O + 2e^-$$

$$E = -0.114 - 0.059\text{pH}$$

$$Fe(OH)_2 + 2OH^- \rightarrow FeO_2^- + 2H_2O + e^-$$

$$E = 0.786 + 0.059\log[FeO_2^-] - 0.118\text{pH}$$

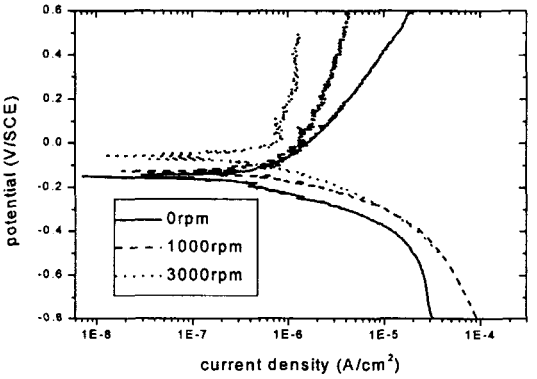

Fig. 10. Effect of Flow Rate on the Passive Film. Water Chemistry is pH 9.8, Oxygenated Condition

Second peak :

$$E(\text{vs. SHE}) = 1.387 - 0.142\text{pH}$$

$$Fe_3O_4 + H_2 + 2OH^- \rightarrow 3(\gamma - FeOOH) + H^+ + 3e^-$$

$$E = 1.916 - 0.019\log P_{H_2} - 0.059\text{pH}$$

$$Fe_3O_4 + 4OH^- \rightarrow 3FeO_2^- + 2H_2O + e^-$$

$$E = 2.411 + 0.177\log[FeO_2^-] - 0.236\text{pH}$$

Fig. 9 shows the polarization result at pH 10.4 with rotating velocity. From the results, it was observed that passive film formation process in active-passive transition region was abrupt with the potential when the rotation rate increases. Suppose that dimension in potential at y-axis can

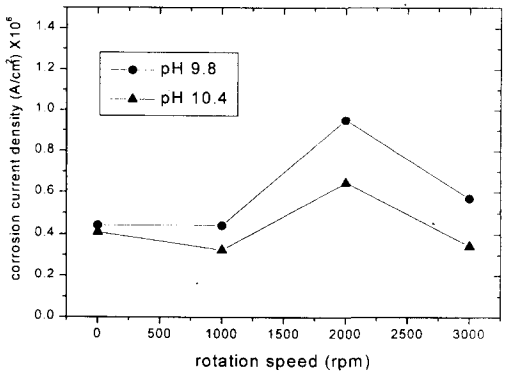

Fig. 11. Results of Linear Polarization with Different pH Condition and Rotating Velocity

be converted into time by dividing scan rate, such a velocity-dependence seems to be the result of acceleration in the precipitation of previously formed hydroxide by the centrifugal force of the RCE. Such result may have relation with the in-situ Mossbauer study of O'Graddy that passive film of steel is usually constituted amorphous iron (III) oxides, iron containing polymeric chains bonded together by binuclear iron compounds containing di-oxy and di-hydroxy bridging bonds between the iron atoms, which were linked by water [11]. The same trend appears in the depassivation stage in Fig. 10 where dissolution current density starts to increase by the weakening of passive film. Current density in high rpm dissolves less than the still condition because the structure of passive film may be dense at depassivation stage as the rotation rate increases.

3.4. Effect of Flow Pattern

Fig. 11 is the result of linear polarization with different pH conditions and rotating velocities. Corrosion current density showed larger value at 1000~2000rpm than at quiescent condition, while it dropped to the initial value at 3000rpm.

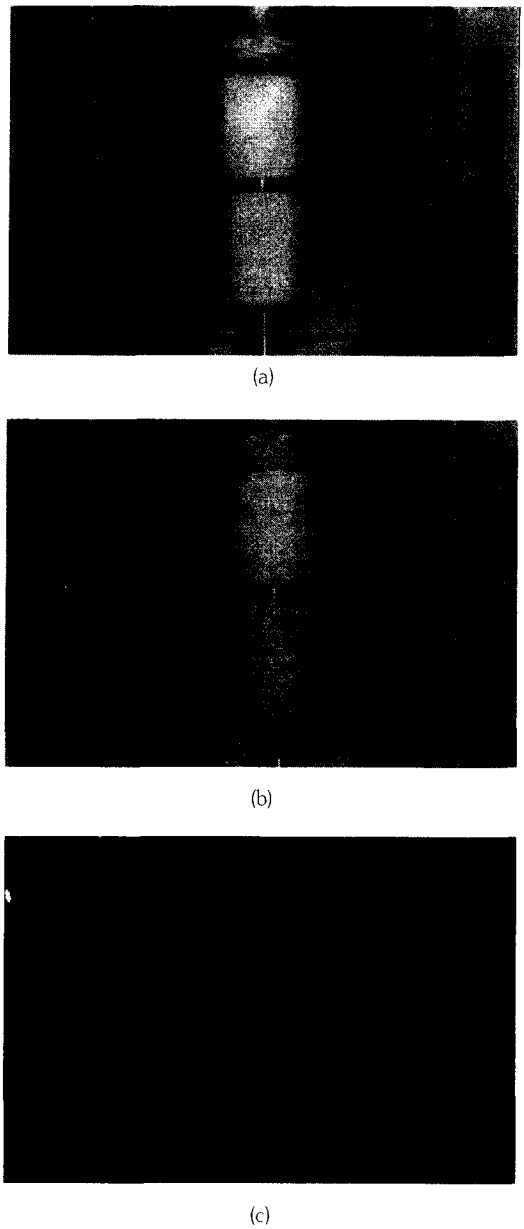

Fig. 12. Flow Pattern of RCE (a) 1500rpm (b) 2500rpm (c) 3000rpm

Fig. 12 is the flow patterns of the given RCE system. From still condition to 1000rpm, no visible change is seen around the rotating cylinder. At 2000rpm small bubbles generated and flowed concurrently near the electrode. Such

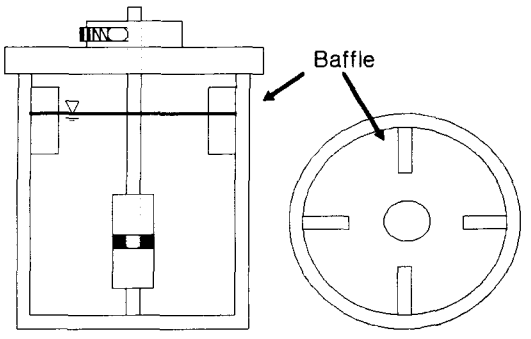

Fig. 13. Baffle Construction to Avoid Taylor Vortices

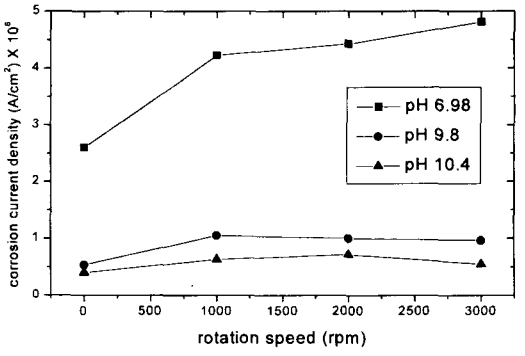

Fig. 14. Linear Polarization Result with Different pH and Rotating Velocities in Baffled Condition

bubbly flow may have an influence on entire corrosion process with a function of mixing action. At 3000rpm, these micro-bubbles coalesced and formed annular flow, caused hindrance against corrosion reaction. Such bubbles may be resulted from the collapse of water blanket generated by Taylor vortices [12].

To avoid generation of bubble and observe pure single phase flow effect on corrosion process, baffle was attached in upper part of RCE cell as in Fig. 13, in which no bubble was formed up to 3000rpm such that corrosion current density did not drop at higher rotating

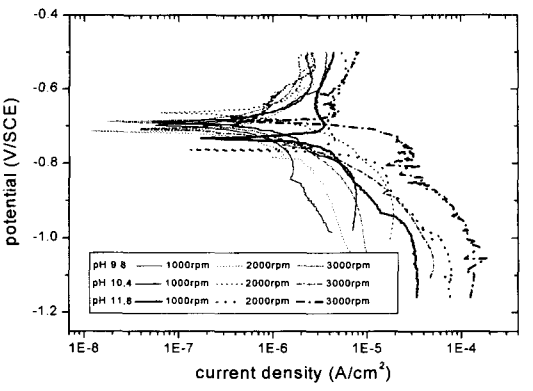

Fig. 15. Cathodic Branch of Polarization Curve in Different pH and Rotating Velocities

speed as expected. Fig. 14 is the result of corrosion current density with different pH and rotating velocities in baffled condition. It more or less increased with the rotating velocity in neutral condition. On the other hand, it soon saturated with the velocity above pH 9.8. It seems that there exists process to control the entire corrosion kinetics regardless of the rotating velocity in alkaline condition. Such result may be coincided with Denpo who measured corrosion rate of carbon steel and 13% chromium alloy in 2% NaCl solution containing CO_2 [13]. He reported that carbon steel, in which passive film did not form, showed great increase of corrosion rate with the rotating speed, whereas 13% Cr steel, in which passive film was apt to generate in open circuit potential, showed saturation of corrosion rate above 1000 rpm.

Limiting current density [14] was measured in cathodic branch to investigate which parameters have a main influence on the entire corrosion process with the rotating velocity. Fig. 15 is the result of limiting current density with the pH and rotating velocity, shows sensitive change with the rotating velocity. Suppose that the governing reaction at cathodic branch rely on the diffusion

process of the reducing species rather than the charge transfer activation process, the whole reaction kinetics of FAC in room temperature alkaline solution can be confined by the activation process which represents formation of the passive film on the bare metal surface. This is consistent with the assumption of the previous FAC model, where it defines that the activation process on the steel surface can make the rate-determining step with the flow velocity to a certain extent [15].

4. Conclusions

1. Corrosion current density decreased up to pH 10.4 but it soon increased with the pH. This is due to the tendency of alkaline corrosion with the increase of half-cell current by the each reacting concentration. One should be careful in extrapolating to higher pH based on the conventional FAC code for CANDU application.
2. Corrosion potential and anodic dissolution current density slightly increased with rotating velocity in neutral condition. This resulted from the diffusion enhancement of the oxidizing agent.
3. Passive film appeared at pH 9.8, its nature became stable from pH 10.4. The formation is based on the mechanisms of oxidation and precipitation of ferrous species into hydroxyl compounds.
4. Corrosion current density increased with the rotating velocity in neutral solution, whereas it soon saturated from 1000rpm above pH 9.8, This seems that activation process, which represents formation of passive film on the bare metal surface, rather than diffusion process, confines the entire corrosion process in alkaline condition.

Acknowledgement

This work was supported by the Brain Korea 21 project

References

1. W. J. Shack, *Proc. of the 3rd International Symposium on Environmental Degradation of Materials in Nuclear Power Systems - Water Reactors, 55* (1988).
2. V. Shah, and P. E. Macdonald, *Aging and Life Extension of Major Light Water Reactor Components, 523* (1993).
3. K. A. Burill, and E. L. Cheluget, *Corrosion of CANDU Outlet Feeder Pipes*, JAIF Int'l Conf. On Water Chemistry, 699 (1998).
4. J. H. Kim and I. S. Kim, *Environmentally Assisted Crack Growth Behavior of SA508 Cl.3 Pressure Vessel Steel*, Proc. of the KNS Spring Meeting, 154, (1998).
5. M. Eisenberg, et al., *Ionic Mass Transfer and Concentration Polarization at Rotating Electrode*, J. of Electrochem. Soc., **101**, 6, 306 (1954).
6. D. A. Jones, *Principles and prevention of CORROSION*, 357 (1992).
7. J. Y. Zou, and D. T. Chin, *Mechanism of Steel Corrosion in Concentrated NaOH Solutions*, Electrochimca Acta, **32**, 12, 1751 (1987).
8. Y. J. Kim, C. C. Lin, and R. Phathania, *Electrochemical Corrosion Potential Measurement with a Rotating Cylinder Electrode in 288℃ Water*, Proc. Of the Water Chemistry of Nuclear Reactors System 6, 139, BNES (1992).
9. J. Y. Zou, and D. T. Chin, *Anodic Behavior of Carbon Steel in Concentrated NaOH Solutions*, Electrochimica Acta, **33**, 4, 477 (1988).

10. T. Misawa, *The Thermodynamic Consideration for Fe-H_2O System at 25℃*, Corr. Sci., **13**, 659 (1973).
11. W. E. O'Graddy, *Mossbauer Study of the Passive Oxide Film on Iron*, J. Electrochem. Soc, **127**, 3, 555 (1980).
12. K. D. Effird, et al., *Correlation of Steel Corrosion in Pipe Flow with Jet Impingement and Rotating Cylinder Tests*, Corrosion, **49**, 12, 992 (1993).
13. K. Denpo and H. Ogawa, *Fluid Flow Effects on CO_2 Corrosion Resistance of Oil Well Materials*, Corrosion, **49**, 6, 442 (1993).
14. M. G. Fontana, *Corrosion Engineering* 3rd edition, 460 (1987).
15. B. Chexal, et al., *Flow-Accelerated Corrosion in Power Plant*, EPRI report TR-106611, 4-33 (1996).